BAMS Article

An Integrated Research Plan for the Tibetan Plateau Land–Air Coupled System and Its Impacts on the Global Climate

Guoxiong Wu, Xiuji Zhou, Xiangde Xu, Jianping Huang, Anmin Duan, Song Yang, Wenting Hu, Yaoming Ma, Yimin Liu, Jianchun Bian, Yunfei Fu, Haijun Yang, Ping Zhao, Lei Zhong, and Weiqiang Ma

ABSTRACT: The unique characteristics of land–air coupling and troposphere–stratosphere interaction over the Tibetan Plateau (TP), the highest landform in the world, play a vital role in weather and climate on regional and global scales. Although a great deal of research has been carried out, large gaps remain in our understanding of TP land–air coupling and its climate effects, due to a lack of observations and the issue of model biases. To address these obstacles, a 10-yr national research program entitled "Changes in the Land–Air Coupled System over the Tibetan Plateau and its Impacts on Global Climate (LASTPIC)" was launched by the National Natural Science Foundation of China in January 2014. What LASTPIC does revolves around three aspects: TP land–air coupled processes; TP's influence on global climate; and reanalysis and model. This paper mainly focuses on the data collection, scientific understanding, and model development of LASTPIC in terms of TP land–atmosphere–ocean coupling and its global climate impacts since program's inception.

KEYWORDS: Atmosphere-land interaction; Climate change; Climate variability

https://doi.org/10.1175/BAMS-D-21-0293.1
Corresponding author: Anmin Duan, amduan@lasg.iap.ac.cn
In final form 14 August 2022

AFFILIATIONS: Wu, Hu, and Liu—State Key Laboratory of Numerical Modeling for Atmospheric Sciences and Geophysical Fluid Dynamics, Institute of Atmospheric Physics, Chinese Academy of Sciences, and University of Chinese Academy of Sciences, Beijing, China; **Zhou, Xu, and Zhao**—State Key Laboratory of Severe Weather, Chinese Academy of Meteorological Sciences, Beijing, China; **Huang**—Collaborative Innovation Center for Western Ecological Safety, College of Atmospheric Sciences, Lanzhou University, Lanzhou, China; **Duan**—State Key Laboratory of Marine Environmental Science, College of Ocean and Earth Sciences, Xiamen University, Xiamen, and State Key Laboratory of Numerical Modeling for Atmospheric Sciences and Geophysical Fluid Dynamics, Institute of Atmospheric Physics, Chinese Academy of Sciences, and University of Chinese Academy of Sciences, Beijing, China; **S. Yang**—School of Atmospheric Sciences, and Guangdong Province Key Laboratory for Climate Change and Natural Disaster Studies, Sun Yat-sen University, Guangzhou, Guangdong, China; **Y. Ma**—Land-Atmosphere Interaction and its Climatic Effects Group, State Key Laboratory of Tibetan Plateau Earth System, Resources and Environment, Institute of Tibetan Plateau Research, Chinese Academy of Sciences, and University of Chinese Academy of Sciences, Beijing, and Collaborative Innovation Center for Western Ecological Safety, College of Atmospheric Sciences, Lanzhou University, Lanzhou, China; **Bian**—Key Laboratory of Middle Atmosphere and Global Environment Observation, Institute of Atmospheric Physics, Chinese Academy of Sciences, and University of Chinese Academy of Sciences, Beijing, and College of Atmospheric Sciences, Lanzhou University, Lanzhou, China; **Fu and Zhong**—School of Earth and Space Sciences, University of Science and Technology of China, Hefei, China; **H. Yang**—Department of Atmospheric and Oceanic Sciences, Fudan University, and Shanghai Scientific Frontier Base for Ocean-Atmosphere Interaction Studies, Shanghai, China; **W. Ma**—Land-Atmosphere Interaction and its Climatic Effects Group, State Key Laboratory of Tibetan Plateau Earth System, Resources and Environment, Institute of Tibetan Plateau Research, Chinese Academy of Sciences, Beijing, and College of Atmospheric Sciences, Lanzhou University, Lanzhou, China

The Tibetan Plateau (TP) accounts for nearly one-quarter of the total land area of China and is the highest plateau in the world. The mechanical and thermal effects of the TP play an important role in the formation of the general circulation pattern, regional weather and climate regimes, multiscale variability of the Asian summer monsoon (ASM), and the global atmospheric energy and water cycle (e.g., Wu et al. 2015; Bian et al. 2020; Fu et al. 2020; Liu et al. 2020). The TP blocks and uplifts the impinging airflows and generates stationary lee waves (Bolin 1950; Yeh 1950). The intense land surface and atmospheric heat source in summer make the TP act as an efficient heat engine to pump warm and moist air from both the Indian Ocean and the western Pacific Ocean, which further greatly enhances the ASM (Wu et al. 1997; Wu and Zhang 1998; Hsu and Liu 2003; Yanai and Wu 2006; Wu et al. 2007, 2012a,b; Liu et al. 2017). Particularly, in parallel with global warming, the TP climate and atmospheric energy budget have also changed significantly over the past several decades, characterized by a striking warming trend and weakened atmospheric heat source (Duan and Wu 2008; Yang et al. 2011). As such, the TP climate system has become a scientific frontier of climate change and Earth system research. Among the multispheric water–ice–air–land–ecosystem–human interactions on the TP, the land–air coupled system acts as a fundamental process in controlling land surface energy partitioning, the atmospheric heat source–sink structure, circulation regime, and hydrological cycle.

On account of its complex terrain, the spatiotemporal characteristics of the atmospheric physical processes over the TP are unique. Since 1979, a series of field experiments over the

TP have been conducted, such as the first Qinghai Xizang Plateau Meteorological Experiment from May to August 1979 (Tao et al. 1986), the second Tibetan Plateau Atmospheric Experiment from May to August 1998 (Chen 1999), the Global Energy and Water Exchange Experiment (GEWEX) Asian Monsoon Experiment on the TP (GAME/Tibet) in the 1990s (Ma et al. 2003), the Coordinated Enhanced Observing Period (CEOP) Asia–Australia Monsoon Project (CAMP) on the TP (CAMP/Tibet) in the 2000s (Ma et al. 2005), the Tibetan Observation and Research Platform during 2004–08 (TORP; Ma et al. 2008), the China–Japan Meteorological Disaster Reduction Cooperation Research Center Project during 2005–09 (Xu et al. 2008), the underway Third Pole Environment (TPE; 2009–present) (Yao et al. 2012), and the ongoing Third Tibetan Plateau Atmospheric Experiment (TIPEX-III), which began formally in 2014 (P. Zhao et al. 2018). Although a large number of valuable land–air exchange datasets have been retrieved together with scientific progress, previous field campaigns on the TP had their limitations in terms of technical conditions and detection equipment capacity. They could not realize an overall design of the three-dimensional system from the land surface processes to the boundary layer, troposphere, and stratosphere, or a synchronous set of observations of different physical processes. It is difficult to objectively describe the complex physical processes of atmospheric vertical structure against the background of multiscale topography and different underlying surface features over the TP. After comprehensively evaluating these previous TP scientific experiments, it is clear that the weakest link is the significant gap in our understanding of the different physical processes between the land surface and the atmosphere over the TP, together with their influence on the weather and climate. Therefore, the difficulty in describing the complex surface physical processes of the plateau seriously hinders improvement in numerical model capabilities with respect to short-term weather forecasting and climate prediction, as well as our understanding of the climate change response.

To address these challenges, a 10-yr national research program entitled "Changes in the Land–Air Coupled System over the Tibetan Plateau and its Impacts on Global Climate (LASTPIC)" was launched by the National Natural Science Foundation of China in January 2014. It is worth noting that LASTPIC focuses not only on scientific perspectives, but also data assimilation and model development, which is a clear difference from previous national plans concerning this region. Moreover, on scientific perspectives, some new topics, such as troposphere–stratosphere interaction, the combined influences from both the TP and the oceans on the Asian monsoon, and the global climate effect of the TP land–air coupled system, have been taken into account. So far, a total of 32 million U.S. dollars has supported 91 projects. This paper aims to present the core scientific issues, project settings, current research progress and future perspectives of LASTPIC.

Core scientific issues

The LASTPIC national research program aims to solve three core scientific issues (Fig. 1):

TP land–air coupled processes. The complex land–air coupled system over the TP includes atmospheric physicochemical processes and their interactions in the boundary layer, the troposphere, and stratosphere. However, owing to the lack of in situ observation data over the TP, there are limitations to our understanding of the multiscale topographic and inhomogeneous thermal forcing, convective systems, surface land–air coupled processes, and three-dimensional fine-scale structure in the tropopause. There are several questions to answer, including the following: How does the complex surface energy balance affect atmospheric structure? What is the nature of the cloud–precipitation physics and atmospheric water cycle processes over the TP? How can the transport processes between the stratosphere and troposphere (in both directions) be analyzed effectively? What is the influence of surface

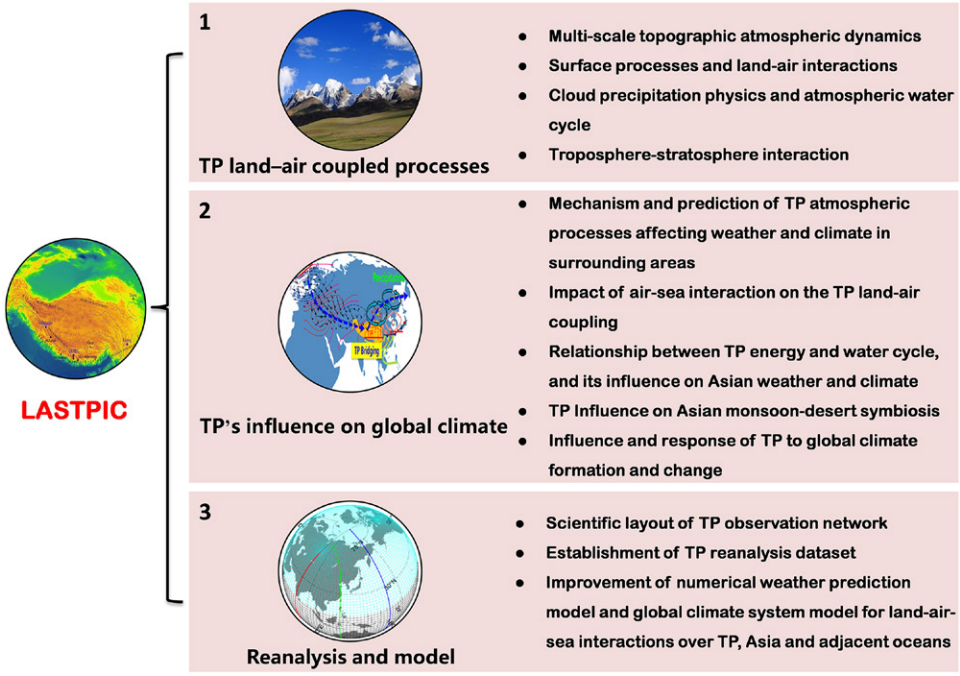

Fig. 1. Core scientific issues to be addressed by LASTPIC, including three aspects: TP land–air coupled processes; TP's influence on global climate; and reanalysis and model.

pollutant emissions on the global stratosphere, through enhanced detection of the three-dimensional fine-scale structure in the tropopause layer over the plateau?

TP's influence on global climate. Although a large number of achievements has been made in this field, there are still many cutting-edge issues that need to be solved urgently. For instance, we need to reveal the mechanism through which the complex multiscale topographic and inhomogeneous thermal effects over the TP influence the regional and global climate variability, understand in detail the TP's atmospheric dynamic processes affecting the Asian monsoon variability, reveal how thermodynamic and mechanical forcings over the plateau influence the Asian monsoon circulation and global climate under the processes of global land–air–sea interaction, quantitatively understand the connection between the TP's energy–water exchange and the Asian monsoon on different time scales, and deepen our understanding of the TP's response to changes in global climate.

Reanalysis and model. Studying the effects of TP weather and climate relies heavily on both observational data and numerical model results. However, observation stations are sparse and unevenly distributed over the TP, and as in situ data have not yet been integrated with most reanalysis data, the observation and reanalysis data can differ greatly from each other in the TP region. Furthermore, the TP's topography cannot currently be described accurately in global climate models because of their coarse horizontal resolutions, which induces false rainfall centers in the eastern part of the TP (Bao and Li 2020). Therefore, the boundary layer schemes of climate models need to be improved for resolving the TP's complex terrain. These problems hinder our understanding of TP climate change and its global impacts, and can even restrict our ability to predict climate disasters in surrounding regions. Thus, there is an urgent demand to strengthen the quality control and assimilation of observation data, and construct an accessible database and sharing platform; to set up a TP reanalysis dataset through the effective integration of observation and global reanalysis data; and to improve the skill of regional weather models and global climate system models with an emphasis on land–air–sea interactions.

Table 1. Type, number, proportion, duration, and funding of projects funded by LASTPIC since its inception.

Type	Number	Proportion (%)	Duration (years)	Funding per project (U.S. dollars)
Management project	3	3	3	750,000
Key project	33	36	4	550,000
"Breeding" project	45	50	3	150,000
Integration project	9	10	3	450,000
Strategy project	1	1	3	600,000

Achievements

So far, the LASTPIC program has funded a total of 91 projects, including 3 management projects, 33 key projects, 45 "breeding" projects, 9 integration projects, and 1 strategy project (Table 1). The percentages are 3%, 36%, 50%, 10%, and 1%, respectively. Aside from the key projects, which have a 4-yr implementation period, all of the other project types have a 3-yr implementation period. The funding is related to the number of participants and missions, as well as the acquisition of observation equipment. It is worth pointing out that LASTPIC pays particular attention to the cultivation of young scientific research talent, as evidenced by the high proportion of "breeding" projects included in the program. The integration projects encourage interdisciplinary research across different teams and scientific fields. Therefore, with such a high output of funding, it is unsurprising that some promising results have been achieved. The following summarizes these achievements funded by the LASTPIC program.

Land–air coupled processes over the TP. The LASTPIC program, in collaboration with the TPE and TIPEX-III experiments, has realized for the first time a comprehensive study of TP atmospheric coupled processes at multiple levels, such as the near surface, boundary layer, troposphere, and stratosphere. In particular, an integrated observational network for multisphere (water–cryosphere–atmosphere–biology) interactions on the TP was formed (Fig. 2; Ma et al. 2017). The LASTPIC is the successor of the programs started earlier including GAME/Tibet (Ma et al. 2005, 2006), CAMP/Tibet (Ma et al. 2005, 2006), TORP (Ma et al. 2008), TPE (Ma et al. 2011), and the national key research program of the study of the changes in the Tibetan Plateau's Climate System and its Impact on East Asia (TPCSIEA; 2010–present; Ma et al. 2017). A part of the stations of LASTPIC are inherited from GAME/Tibet, CAMP/Tibet, TORP, TPE, and TPCSIEA (Table 2). This network contains 9 multisphere stations, 11 multisphere sites, 3 soil moisture and soil temperature networks, and 5 radiosonde stations. Each multisphere station includes an atmospheric boundary layer tower (or an automatic weather station), a four-component radiation measurement system, a five-level soil moisture and temperature measuring network, a sonic turbulent measurement system, a CO_2–H_2O flux measurement system, and a microwave radiometer. The monitoring network covers most parts of the TP, and the observation period is long and continuous. It should be mentioned that most of our comprehensive observation and research stations and observational sites are totally different from those in P. Zhao et al. (2018), which is shown in Table 2 in detail. In other words, these two observation networks provide invaluable, complementary datasets for the promotion of Tibetan meteorological research, especially for the implementation of LASTPIC.

Based on the integrated network platform, a long-term hourly dataset (Table 3) on the TP covering the period 2005–16 has been collected and released at the National Tibetan Plateau/Third Pole Environment Data Center (X. Li et al. 2020) aiming for illustration of the land–atmosphere interaction characteristics. The 2005–16 data in this study also include the observations conducted in TORP and TPCSIEA, lasting for 12 years with a fine temporal

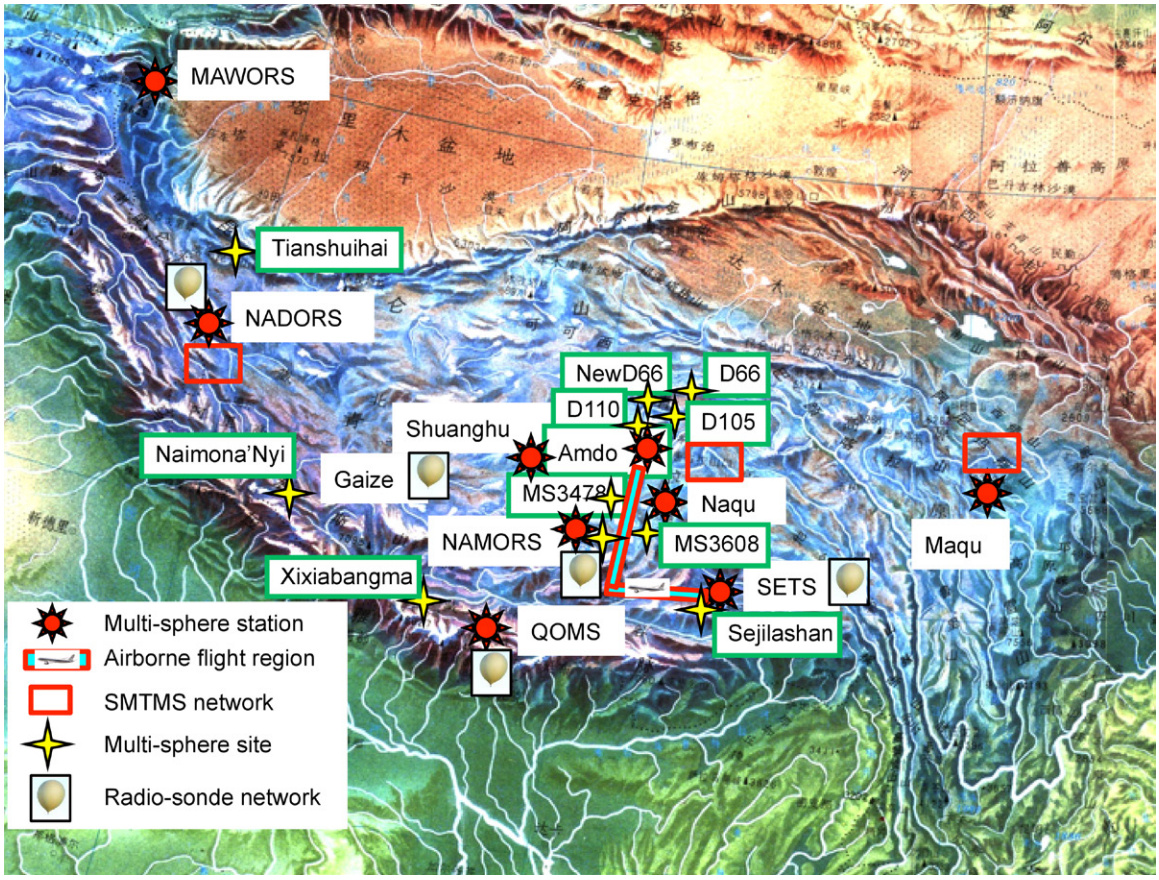

Fig. 2. The integrated observational system for multisphere (water–cryosphere–atmosphere–biology) interactions over the TP (modified from Ma et al. 2017).

resolution of 30 min. This dataset is accessible to the scientific community worldwide via https://doi.org/10.11888/Meteoro.tpdc.270910. It should be noted that among the released observation datasets for the land–air coupled system over the TP, this one has the highest temporal resolution so far. Due to this improvement in the TP observation network, the resultant observational evidence has helped us to further reveal the mechanisms of the land–air coupled system over the TP and its effects on weather and climate.

Table 2. Stations of LASTPIC, its inheritance from GAME/Tibet, CAMP/Tibet, TORP, TPE, TPCSIEA, and its difference from TIPEX-III.

Project	Starting year	Stations	Reference
GAME/Tibet	1996	Anduo, D66, D105, D110, MS3478, MS3608, MS3637, Naqu, NODA, Tuotuohe, WADD	Ma et al. (2006)
CAMP/Tibet	2001	Anduo, ANNI, BJ, D66, D105, D110, MS3478, MS3608, MS3637, Naqu, NODA, Tuotuohe, WADD	Ma et al. (2006)
TORP	2005	BJ, MAWORS, NADORS, NAMORS, QOMS, SETORS	Ma et al. (2008)
TPE	2009	Gongga, Haibei, Lhasa, MAWORS, NADORS, NAMORS, QOMS, SETORS	Yao et al. (2012)
TPCSIEA	2010	Amdo, D66, D105, D110, Gaize, Maqu, MAWORS, MS3478, MS3608, NADORS, Naimona'Nyi, NAMORS, Naqu, NewD66, QOMS, Sejilashan, SETS, Shuanghu, Tianshuihai, Xixiabangma	Ma et al. (2017)
LASTPIC	2014	Amdo, D66, D105, D110, Gaize, Maqu, MAWORS, MS3478, MS3608, NADORS, Naimona'Nyi, NAMORS, Naqu, NewD66, QOMS, Sejilashan, SETS, SHCEOR, Sino-Nepal, Tianshuihai, Xixiabangma	This paper
TIPEX-III	2014	Anduo, Bange, Biru, Dali, Jiali, Linzhi, Namucuo, Naqu, Nierong, Shiquanhe, Wenjiang	P. Zhao et al. (2018)

Land surface processes over the TP. Accurate estimation of land surface heat fluxes (LSHFs) over the TP is critical for studying the energy and water cycles. Against the background of global warming, a decreasing trend in surface sensible heat flux (SH) contributes to the weakening trend in the TP atmospheric heat source (Duan et al. 2013). Conversely, the latent heat flux shows an increasing trend over most of the TP, according to a recently released dataset of surface energy balance components from 2001 to 2012 (Han et al. 2017). This can be attributed to the increase in rainfall and vegetation greening (Zhong et al. 2019a). In recent years, remote sensing retrievals of LSHF in the TP domain have undoubtedly improved on different spatiotemporal scales. In particular, Zhong et al. (2019b) first estimated hourly LSHFs for the entire TP through the combined use of polar-orbiting and geostationary satellite data (Fig. 3). This dataset of hourly LSHFs was validated and showed good agreement with the in situ measurements from the established integrated observational network platform (Zhong et al. 2019b). It offers distinct advantages over the flux products derived from the Global Land Data Assimilation System (GLDAS). Thus, this hourly LSHF dataset can help in detecting the diurnal variation in the atmospheric boundary layer of the TP.

Table 3. Summary of the long-term hourly dataset of integrated land–atmosphere interaction observations on the TP for the period 2005–16 (https://doi.org/10.11888/Meteoro.tpdc.270910**).**

Stations	Variables	Units
BJ, QOMS, SETORS, NADORS, MAWORS, NAMORS	Air temperature	°C
	Wind speed and direction	m s^{-1}
	Humidity	%
	Relative humidity	%
	Water vapor pressure	kPa
	Pressure	hPa
	Radiations	W m^{-2}
	Precipitation	mm
	Soil temperature	°C
	Soil moisture	υ/υ %
	Soil heat flux	W m^{-2}
	EC	—

The most obvious feature of the TP is the land surface occupied by frozen soil. The thawing of frozen soil can significantly affect the soil water content and energy budget, and subsequently other land surface processes over the TP, further influencing the land–air interactions over and around the TP region. Combining soil moisture data from GLDAS, version 2, and agricultural meteorological stations of the China Meteorological Administration (CMA), Yang and Wang (2019a) pointed out that a drier surface can be expected in the after-thaw period (spring) due to enhanced evaporation, if there is no soil freeze–thaw process. This indicates that the freeze–thaw process has a water-storage effect. Furthermore, the freeze–thaw process can induce soil moisture anomalies that persist into the summer, which will enhance the thermal forcing of the TP, leading to variation in the subtropical westerlies and the propagation of a stationary Rossby wave train in the midlatitudes, as evidenced by site observations and numerical experiments (Yang and Wang 2019b).

Cloud and precipitation. With the development of ground stations and remote sensing over the TP, the spatial patterns and diurnal variation of cloud systems have been steadily revealed by LASTPIC. Recently, a new platform has been provided for studying the diurnal variations of cloud macroparameters, and establishing inversion algorithms based on cloud microparameters, such as cloud water and ice content (Zhao et al. 2017; Gao et al. 2018). Furthermore, it was found that the TP's terrain has a significant compression effect on cloud thickness and layers (Yan and Liu 2019).

The TP vortex is a low pressure synoptic system that consistently appears in the midtroposphere over the TP. Moreover, it can interact with the Southwest China vortex—the most representative weather system on the leeward slope of the TP—causing rainstorms or other weather disasters. However, the processes of interaction between the TP vortex

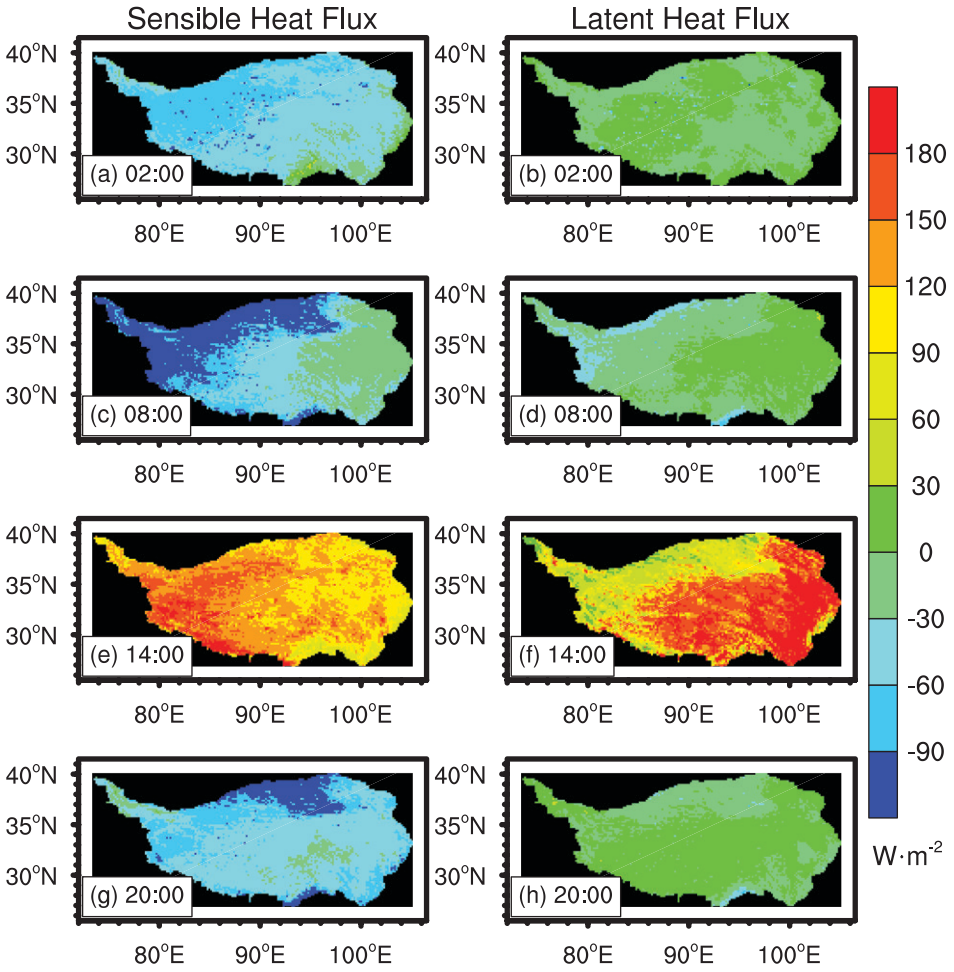

Fig. 3. Annual mean spatial distribution and diurnal cycle of (a),(c),(e),(g) sensible heat flux and (b),(d),(f),(h) latent heat flux in 2008 over the TP (modified from Zhong et al. 2019b).

and Southwest China vortex had not been very clear until a recent experiment funded by LASTPIC. The experiment involves time-intensive observations, clearly revealing the initial state, the movement, and interaction of these two vortices—especially the merging processes that combined two vortices, the influences of cold and warm advection, and the subsequent rainstorms (Cheng et al. 2016). In particular, the distribution of vorticity of the combined vortex is very similar to that of the Southwest China vortex, while the distribution of temperature is basically the same as that of the TP vortex. None of this evidence is available from conventional observation data.

The rainstorms that occur over the Yangtze River basin (YRB) in summer, which can result in severe flooding and losses to human life and property, are strongly influenced by TP convection systems. The heavy rains over the YRB are mainly caused by the eastward movement of clustered convection systems from the central part of the TP (Hu et al. 2016). The close relationship between TP convection systems and YRB rainstorms was also confirmed by regional Weather Research and Forecasting (WRF) Model simulations and Lagrangian backward-trajectory tracking in recent LASTPIC-funded studies (Zhao et al. 2019a,b). The model simulations also pointed out that a three-dimensional water vapor flux–vortex coupled structure links the convection systems in the central TP to the rainstorms in the YRB, accompanied by low-layer convergence and high-level divergence.

Troposphere–stratosphere interaction. Troposphere–stratosphere interaction is strongly influenced by the circulation of the ASM. Pollutants from the surface are transported upward to the upper troposphere and lower stratosphere (UTLS) through frequent deep convection,

where they become trapped by the South Asian high (SAH). When the ASM prevails, deep convection events comprise localized thunderstorms overland and severe tropical cyclones over the western Pacific Ocean. Based on balloonborne measurements over Kunming, China, funded by LASTPIC, it was demonstrated that strong tropical cyclones carry ozone-poor air from the ocean surface to the UTLS and into the SAH via quasi-horizontal advection (D. Li et al. 2020). Due to the trapping effect of the SAH, some pollutants mix horizontally within, and stay for a long period. Nevertheless, some will leave the SAH and enter the stratosphere via one of the following two ways. The first and most important way is across the isentropic surface and into the tropical stratosphere via a slow diabatic uplift motion, mostly occurring over the southern part of the SAH (Fan et al. 2017). Approximately two-thirds of the transport into the stratosphere takes place in this way. The second way is isentropic transport via eddy shedding over the northern and eastern parts of the SAH, which is conducive to air accessing the subtropical stratosphere (Fan et al. 2017) and is crucial for changes in stratospheric composition.

In addition to dynamical troposphere–stratosphere transport processes, the chemical reactions of pollutants over the ASM region during transport have also been reported. In the UTLS, a significant aerosol layer within the SAH that occurs every summer was discovered, often referred to as the Asian tropopause aerosol layer (ATAL; Vernier et al. 2011). A series of internationally coordinated research funded by the LASTPIC program provided new evidence that the TP acts as an important pathway for troposphere–stratosphere interaction. Based on a combination of in situ aerosol-size spectral measurements and numerical modeling, Yu et al. (2017) pointed out that a significant amount of particle formation is generated within the SAH over the TP, and pollutants emitted from Asia contribute significantly to the stratospheric aerosol budget in the Northern Hemisphere through the TP pathway (Fig. 4). After entering the UTLS, pollutants accumulate and go

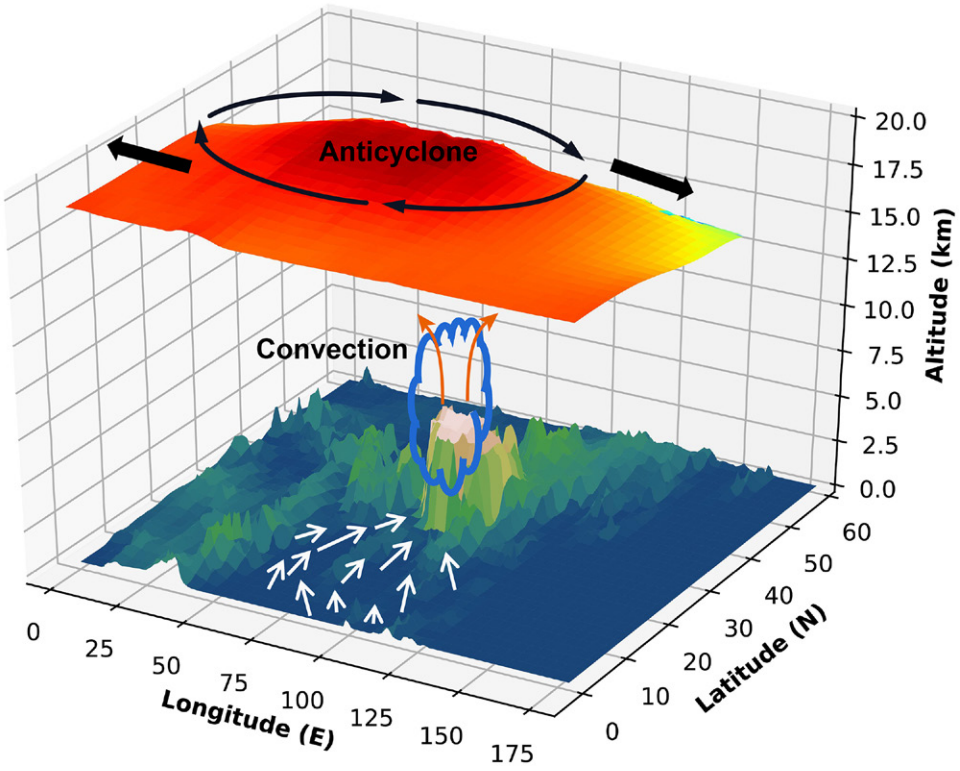

Fig. 4. Schematic diagram showing the transport of air during the ASM. The ASM dome is the higher tropopause heights denoted by red colors. Updrafts are denoted by orange arrows. Surface wind is denoted by white arrows. This figure was produced by Dan Li and Jianchun Bian from LAGEO, IAP/CAS, based on the concepts of Park et al. (2009) and Yu et al. (2017).

through a series of chemical changes in a reactive reservoir, and the reaction products are dispersed around the globe (Lelieveld et al. 2018).

LASTPIC-funded research has also explored the formation of aerosols and their composition in the ATAL via model applications. Using a global three-dimensional Goddard Earth Observing System chemical transport model, Gu et al. (2016) showed that the contribution rate of nitrate to the ATAL could be as high as around 60% at 100 hPa during the summertime over the TP and the South ASM region. Further studies have revealed that the existence of mineral dust in the ATAL cannot be ignored either, also indicating that the TP's UTLS can serve as a clear conduit for natural and anthropogenic gases and aerosols into the stratosphere (Ma et al. 2019). Therefore, strong troposphere–stratosphere interactions occurring over the TP have a critical effect on the global climate via chemical, microphysical and radiative processes, due to the TP's high elevation.

TP's influence on global climate. In-depth investigations into the variation of the TP climate and its global climate impacts on multiple time scales have progressed to yield fruitful advancements. In particular our understanding of the climate dynamics of the TP has developed considerably since the 1980s, with rapid progress having been made through both observational and numerical modeling results. From different perspectives, such as energy, potential vorticity, and angular momentum conservation theories, LASTPIC-funded studies have confirmed that it is the TP's heating rather than its role as a thermal isolator separating tropical and extratropical air masses that plays the dominant role in the formation of the ASM circulation. Also, the LASTPIC program has helped to significantly advance scientific understanding of TP weather and climate effects in terms of land–air–sea interaction in Earth's climate system.

TP THERMAL FORCING AND ITS INFLUENCE. The TP presents as an atmospheric heat source in boreal summer but a heat sink in boreal winter. In quantitative studies, the atmospheric heat source, a net heat gain (loss), is defined as the sum of SH, the latent heat released to the atmosphere via precipitation (LH) and the net radiation flux of the air column (RC) at a given location during a given time period. In general, SH is dominant in spring over the TP. With the wet season coming, LH starts to increase in May, exceeds the SH in late May and early June, and finally reaches its maximum in July (Y. Zhao et al. 2018). In contrast, RC shows a cooling effect throughout the whole year but with an obvious annual cycle. Aside from the atmospheric heat source and its components presenting seasonality, they also depend on the terrain height regardless of season (Yu et al. 2018). It is worth noting that the increase in SH with elevation is of great significance in forcing atmospheric circulation.

LASTPIC-funded work has proposed an updated mechanism for the thermal impacts of the Tibetan–Iranian Plateau (TIP) on the formation of the ASM (Liu et al. 2017, 2020). In every summer, the SH over the TIP coupled system causes strong upward motion over the region and brings sufficient water vapor transport from the oceans to land, subsequently influencing the formation of ASM precipitation. This is often referred to as the sensible heat–driven air pump (SHAP). Although the effects of SH over the Iranian Plateau and TP on the climate of other regions can be mutually reinforced or offset (Liu et al. 2017), the interaction between SH and LH over the TP is dominant in this TIP coupled system. In addition, the onset of the ASM is strongly affected by the thermal forcing of the TP, especially for the earliest ASM onset occurring in the eastern Bay of Bengal (BOB). The spring TP heating forces a cyclonic gyre to the south of the TP. The cyclonic gyre leads to the SAH moving northwestwards with its center located in the northern Indochina Peninsula, inducing intensified divergent flow over the southeastern BOB. Consequently, the in situ vorticity is reduced aloft and an air-pumping mechanism is formed. Furthermore, the cyclonic gyre also causes the occurrence of a distinct

warm pool in the BOB that stimulates the development of convection in situ. The coupling of the BOB convection with the vorticity minimum aloft along with the air pumping ultimately triggers the first ASM onset in the southeastern BOB (Wu et al. 2015). As for the interdecadal variability of ASM rainfall, the decrease in TP SH in spring and summer is responsible for the generation of an anomalous rainfall pattern with a north–south seesaw axis over East China, which is often referred to as the "south flood–north drought" pattern (Wu et al. 2017).

Scientific discussion is key for scientific progress. A debate on the maintenance of the South Asian monsoon (Qiu 2013) was sparked by the study of Boos and Kuang (2010) in which a new hypothesis was raised that challenged traditional TP thermal forcing theory, as follows: The Himalayas act as a thermal isolator to prevent the cold and dry northerlies from entering the tropics, while the high-entropy air in the lower troposphere over India can be directly coupled to the upper-level warm center via monsoon convection (Boos and Kuang 2010). However, results in LASTPIC-funded studies contradict this view. Due to astronomical factors and the TP's location, the summertime prevailing wind in the lower troposphere over the TP is southerly rather than northerly, and thus there is no cold northerly advection. This indicates that the TP does not act as a thermal isolator to prevent the invasion of cold and dry air from the north (He et al. 2015). LASTPIC studies have also found that descending air dominates the region beneath the upper-level warm center and the SAH, while strong convections are located to the south of the warm center in association with the tropical convergence zone, and to its north in association with the uplifted transport of water vapor along the southern slope of the TP. Moreover, a large amount of water vapor transported from the Arabian Sea and BOB benefits the formation of a surface entropy maximum over India, which is implemented by the TIP thermal pumping mechanism (He et al. 2015). Therefore, the maintenance of the ASM is basically controlled by both the land–sea thermal contrast and the elevated heating of the TP.

LASTPIC-funded research has revealed that the TP can also influence upstream climate variability. The rainfall variability over the central-eastern Sahel is closely related to the tropospheric temperature over the TP in boreal summer, which could be explained by an anomalous zonal–vertical cell with ascent over the western TP and descent over the Mediterranean Sea, and an anomalous meridional–vertical cell rising over the Sahel (Nan et al. 2019). And beyond that, TP heating also exerts a strong influence on the climate over other upstream regions such as the North Atlantic, southern Europe, North Africa, and West Asia, as determined by a series of model experiments (Lu et al. 2018). As a result of the TP SHAP effect, the TP heating induces warming and anomalous upward motion, as well as the generation of a low-level cyclone and a high-level anticyclone in situ. The corresponding intensification of the SAH and Atlantic subtropical high accompanied by decreased rainfall over the Mediterranean Sea and extratropical North Atlantic occurs via the processes of a Rossby wave response and thermally driven vertical cell. Although the TP covers only one-quarter of the Chinese land area, the TP heating accounts for about a half of the climate signals caused by the whole Asian continent's heating, as measured by relative changes in circulation patterns, precipitation, and surface temperature (Lu et al. 2018).

Some of the very latest research funded by LASTPIC have pointed out that, although sensible heating is a crucial process of TP thermal forcing, the SH over the TP is inadequate for use as a measurement of TP thermal forcing in climate diagnostic studies, particularly in the rainy season. This is because it receives strong feedback from precipitation; plus, the expression cannot successfully capture the elevated topographic effect and combine both the thermal and dynamical forcing of the TP (He et al. 2022). He et al. (2022) further proposed a new index based on the potential vorticity framework, which comprehensively considers the elevated, thermal, and dynamical effects of the TP. They demonstrated that the TP surface potential vorticity (SPV) could capture the thermodynamical forcing of the TP well during boreal summer, and has a better relationship than SH with the seasonal

variation of the ASM (Fig. 5). Their results suggest that the transition of TP forcing from a cooling to heating source takes place in April, and the SPV reaches a maximum from June to August, which is consistent with the evolution of the ASM precipitation. Further studies (Sheng et al. 2022; Yu et al. 2021, 2022) have revealed that the TP's SPV is important for regulating the precipitation pattern of the East Asian monsoon during boreal summer, the seasonal transition of the South ASM during boreal spring, and El Niño–Southern Oscillation during the following winter.

Connection between TP and remote oceans. As a critical forcing source for affecting global atmospheric and oceanic circulations, the TP is also influenced by remote oceans via Rossby waves, the westerly jet, local atmospheric responses, and teleconnections. In recent decades, the relationship of the TP with the oceans and their synergistic effect on the Asian monsoon have attracted increasing attention. In this part, two aspects of the research progress made by LASTPIC will be described: the connection between TP and the remote oceans, and their synergistic impact on the East ASM (EASM).

For the Pacific Ocean, the spring surface sensible heating over the TP can lead to a change in the sea surface temperature (SST) of the equatorial Pacific Ocean and then modulate the western Pacific subtropical high, as revealed by a general circulation model (GCM) experiment (Duan et al. 2017). Moreover, the spring TP thermal forcing stimulates the generation of an anomalous atmospheric circulation with barotropic structure over the North Pacific (Sun et al. 2019). Consequently, due to the sea surface heat exchange and Ekman transport, the underlying SST has changed obviously. It is worth noting that the effect of the TP spring thermal forcing on the North Pacific operates on the interannual time scale.

For the Indian Ocean, the TP thermal effect in boreal summer can significantly reduce the SST over the northern Indian Ocean through the prevailing southwesterlies, and thus suppress monsoonal convections in situ (Wang et al. 2018). More importantly, He et al. (2019b), based on a comparison of experiments between an atmospheric GCM and a coupled GCM, revealed that the response of air–sea coupling processes tends to counteract the impact of the TIP thermal forcing on the surrounding circulation. Moreover, the influence of the Indian Ocean Basin mode (IOBM) significantly changes the heating conditions of the TP via an alteration of the local meridional circulation (Y. Zhao et al. 2018).

Through air–sea interaction, the North Atlantic SST variation is closely connected to the TP heating by the existence of a stationary wave train across Eurasia, which may in turn moderate the TP thermal impact (Cui et al. 2015; Yu et al. 2021). By comparing the TP heating

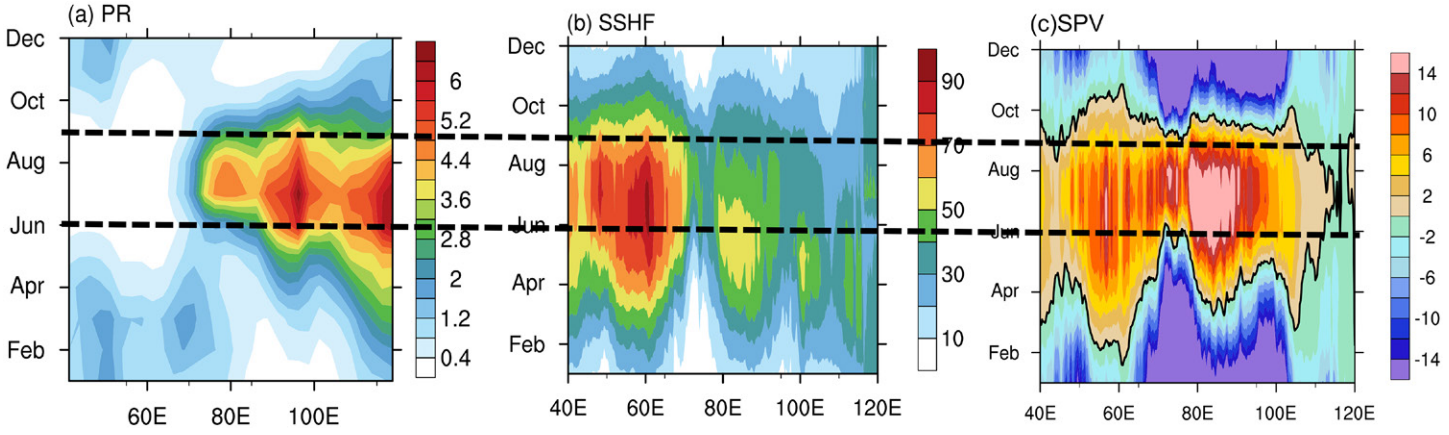

Fig. 5. Climatological (1979–2014) annual cycle (25°–40°N mean, and where the elevation is above 500 m) of (a) precipitation (mm day^{-1}) from GPCP, (b) SH (W m^{-2}), and (c) the SPV (PVU) from ERA5. The bold black dashed lines denote the period of June–August. This figure was produced by Bian He from LASG, IAP/CAS.

experiments with and without Atlantic SST variation, it was found that more than 20% of the upstream climate signal caused by the TP thermal effect is regulated by the variation in the Atlantic SST (Lu et al. 2019). Moreover, the difference between these two experiments demonstrated that if the Atlantic SST variation is included, an anomalous wave train will be generated with three maximum geopotential height centers located in the North Atlantic, Arctic Ocean, and to the east of Japan, and four minimum geopotential height centers over the mid-Atlantic, northern Europe, northeastern North America, and the northwestern Pacific. This induces changes in circulation and rainfall patterns over the TP's upstream regions, particularly a weakening of the TP thermal-induced rainfall dipole over West Africa and the tropical eastern Atlantic.

Figure 6 summarizes the influence of atmospheric anomalies associated with thermal forcing by the TP on the interannual variability of remote SST anomalies in February–May as revealed by LASTPIC studies. In early spring (February–April), a tripole SSTA mode appears over the North Atlantic, of which the warm core can stimulate a Rossby wave train propagating eastward and affect the TP with the enhanced westerly jet (Cui et al. 2015; Yu et al. 2021). In late spring (May), the positive IOBM induces descending motion over the southeastern TP through triggering an anomalous Hadley-type meridional cell between the Indian Ocean and the TP, subsequently resulting in reduced precipitation and heating over the TP (Y. Zhao et al. 2018). In turn, the spring (March–May) TP heating anomaly can influence the North Pacific Ocean SST and mixed layer temperature. The abnormal TP sensible heating can generate a downstream Rossby wave train and form an anomalous equivalent barotropic anticyclone over the North Pacific, resulting in SST anomalies and the mixed layer temperature presenting a horseshoe-like pattern through altering the net heat fluxes and Ekman transport (Duan et al. 2017; Sun et al. 2019).

In addition to the SST pattern, paleoclimatic evidence has suggested an importance of the TP in the generation of the remote Atlantic meridional overturning circulation (AMOC) (Fallah et al. 2016). A recent study funded by LASTPIC employed a fully coupled climate model to reconfirm that the AMOC would collapse without the presence of the TP (Yang and Wen 2020). The collapse of the AMOC is shown as an obvious reduction in the downward

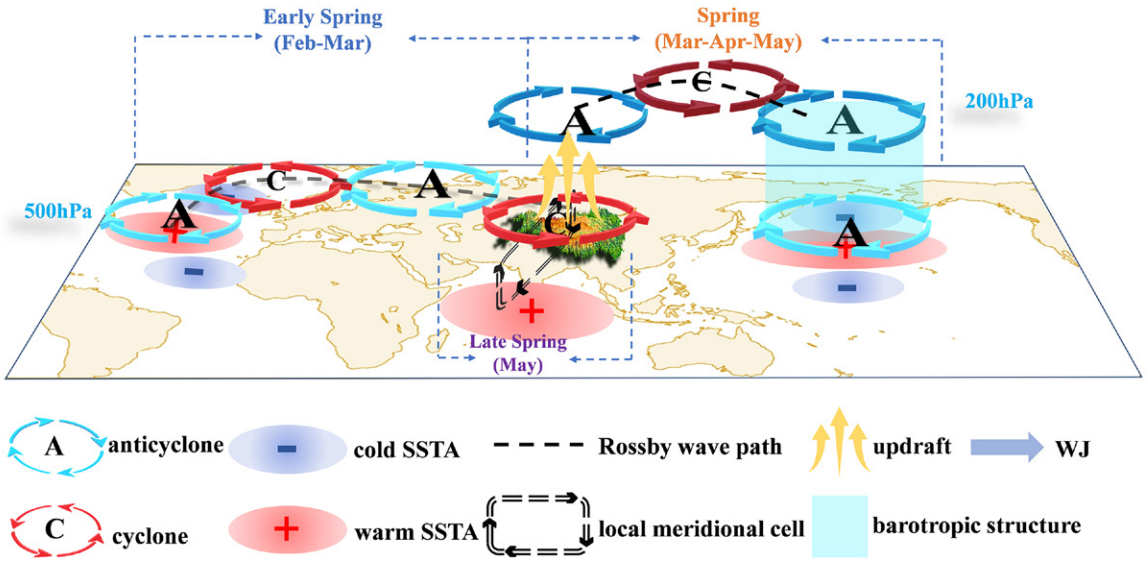

Fig. 6. Schematic diagram of the influence of atmospheric anomalies associated with thermal forcing by the TP on the interannual variability of remote SST anomalies in February–May. In early spring (February–March), the warm center of a tripole SST mode over the North Atlantic can stimulate a Rossby wave train to propagate eastward and affect the TP. In late spring (May), the positive IOBM results in reduced precipitation and heating over the TP. In turn, the spring (March–May) TP heating anomaly can influence the North Pacific Ocean SST and mixed layer temperature.

mass transport in the subpolar North Atlantic. It takes 300–400 years for the AMOC to reach a quasi-equilibrium state in response to the TP's removal, and its final intensity is reduced by 90%. The mechanism responsible for the effects of the TP on the AMOC was given by Yang and Wen (2020), in which the transient change of the AMOC was investigated in detail. In addition, it was suggested that the Pacific meridional overturning circulation would be established alongside the collapse of the AMOC. The uplift of the TP appears to play a critical role in the seesaw pattern of change in the Atlantic and Pacific overturning circulations (Figs. 7a,c). In short, the TP influences the oceanic circulation and deep-water formation of the North Atlantic and North Pacific mainly through atmospheric processes. The key factor that triggers the weakening of the AMOC is the anomalous atmospheric moisture transport from the tropical Pacific to the North Atlantic (Fig. 7b). Due to the relocation of the global water vapor transport in response to the TP's removal, the deep-water formation switches from the North Atlantic (Fig. 7a) to the North Pacific (Fig. 7c).

LASTPIC-funded research has pointed out that the interannual variability of the EASM is controlled by both the TP thermal forcing and the IOBM (Hu and Duan 2015). Above-normal TP thermal forcing induces an enhancement of the SAH in the upper troposphere and the northerly (southwesterly) winds over northern (southern) China in the lower troposphere. This configuration ultimately strengthens the main precipitation belt of the EASM. The positive phase of the IOBM benefits the generation of an anomalous anticyclone over the northwestern Pacific in the lower layer, which is consistent with the EASM's dominant mode of circulation. Thus, excessive EASM rainfall can be attributed to the occurrence of both an IOBM positive phase and above-normal TP thermal forcing.

Reanalysis and model. With the rapid increase in the availability of in situ observations and information inferred from satellite data, how to assimilate such newly obtained observations into numerical models for better weather forecasting and climate prediction is imminently achievable. Thus, the third step for LASTPIC's implementation is to strengthen the quality control and assimilation of observation data, to set up a TP reanalysis dataset, and to improve the skill of numerical models. To date, the LASTPIC program has partly funded the establishment of a data assimilation system [CMA Land Data Assimilation System V2.0 (CLDAS-V2.0)]

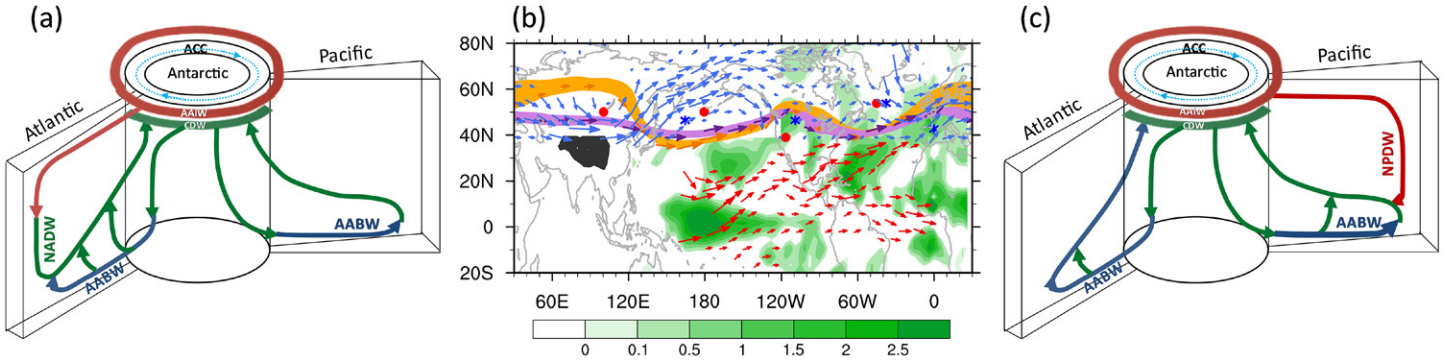

Fig. 7. Schematic diagram showing the global overturning circulation and the TP's effect on global moisture transport. (a) A simplified version of the current global overturning circulation, after Schmitz (1996). (b) The changes in the westerlies and water vapor transport in the Northern Hemisphere after the TP is removed. The brown and purple ribbons and arrows show the stationary wave structure and corresponding winds at 850-hPa geopotential height under realistic continental topography (Real) and the situation when the TP is removed (NoTibet). Blue arrows show the wind changes in NoTibet with respect to Real. Red arrows and green shading represent the changes in vertically integrated water vapor transport and convergence in NoTibet with respect to Real. The TP is indicated by the gray patch. More details can be found in Yang and Wen (2020). (c) The global overturning circulation when the TP is removed.

and related hourly reanalysis datasets, and the development of a new version of the high-resolution version of the Flexible Global Ocean–Atmosphere–Land System model, finite-volume version 3 (FGOALS-f3-H).

Reanalysis data. The assimilation system CLDAS-V2.0 was developed at CMA, and LASTPIC has funded several projects for its development. It fuses station observational data from nearly 60,000 automatic weather stations in China and multiple satellite integrated datasets over East Asia, including those of *Fengyun-2E*/*G*, Fengyun-3, the Tropical Rainfall Measuring Mission Microwave Imager (TRMM/TMI), Microwave Humidity Sounder *NOAA-18*/*-19*, and Defense Meteorological Satellite Program (DMSP)-*F16*/*-17*/*-18* (Han et al. 2019). CLDAS-V2.0 is now operational at the CMA and a corresponding real-time product dataset of CLDAS-V2.0 has been generated. This real-time dataset is an hourly grid-fusion analysis product covering the Asian region (0°–65°N, 60°–160°E) with a high horizontal resolution of 0.0625° × 0.0625°, including six atmospheric driving field products (2-m air temperature, 2-m specific humidity, 10-m wind speed, ground pressure, precipitation, and shortwave radiation), a ground temperature analysis product, a soil moisture analysis products (five layers: 0–5, 0–10, 10–40, 40–100, and 100–200 cm), a soil temperature analysis product (five layers: 5, 10, 40, 100, and 200 cm), and a soil relative humidity analysis product (three layers: 0–10, 0–20, and 0–50 cm). It can be freely downloaded from http://data.cma.cn/en/?r=data/detail&dataCode=NAFP_CLDAS2.0_RT.

Within the framework of CLDAS, an hourly multisource precipitation fusion dataset for China (CLDAS-Prcp) has been produced via temporal downscaling and multigrid variational analysis (Sun et al. 2020). This dataset covers the period of 1998–2018 with a horizontal resolution of 6.25 km. Dependent evaluation shows that CLDAS-Prcp performs better within China than multiple precipitation datasets, while independent evaluation indicates that the simulation of snow depth driven by CLDAS-Prcp is far superior to that driven by CLDAS-V2.0 precipitation. The improvement of snow depth data are beneficial to the study of TP snow cover and its impacts on climate. In addition, hourly reanalysis datasets of soil moisture, soil temperature, surface temperature and snow cover in China, with a spatial resolution of 0.0625° from 1998 to the present day, have been developed in historical and real time. Figure 8 shows the bias and root-mean-square deviation of the soil surface temperature in CLDAS and GLDAS, which implies that the product quality of CLDAS is better than that of its international counterpart (i.e., GLDAS). The main difference between CLDAS and GLDAS is that CLDAS includes the 60,000 automatic weather station observations in China but GLDAS does not and CLDAS uses a better high-resolution model for the data assimilation. The above reanalysis data are still being optimized and will be available to scientists in due course.

Model development. A new version of the high-resolution climate system model FGOALS-f3-H with a horizontal resolution of 25 km was developed. Several parameterization schemes were adjusted or implemented in this version to take the features of TP air–land processes into account. First, a convection-resolving precipitation parameterization—the resolving convective precipitation scheme—was developed to reduce the precipitation bias, especially along the southern slope of the TP (Bao and Li 2020). Second, a Monte Carlo three-dimensional radiation scheme (Lee et al. 2013) was implemented in FGOALS-f3-H to consider the shadow effects and multiscattering between adjacent terrain due to the complex topography over the TP. Third, the *K*-profile parameterization was coupled to the lake module in FGOALS-f3-H to better simulate the vertical mixing processes in TP lakes (Zhang et al. 2019; Zhu et al. 2020).

By implementing these changes, the new version of FGOALS-f3-H and the corresponding low-resolution FGOALS-f3-L with a horizontal resolution of 100 km (FGOALS-f3-L/H in short)

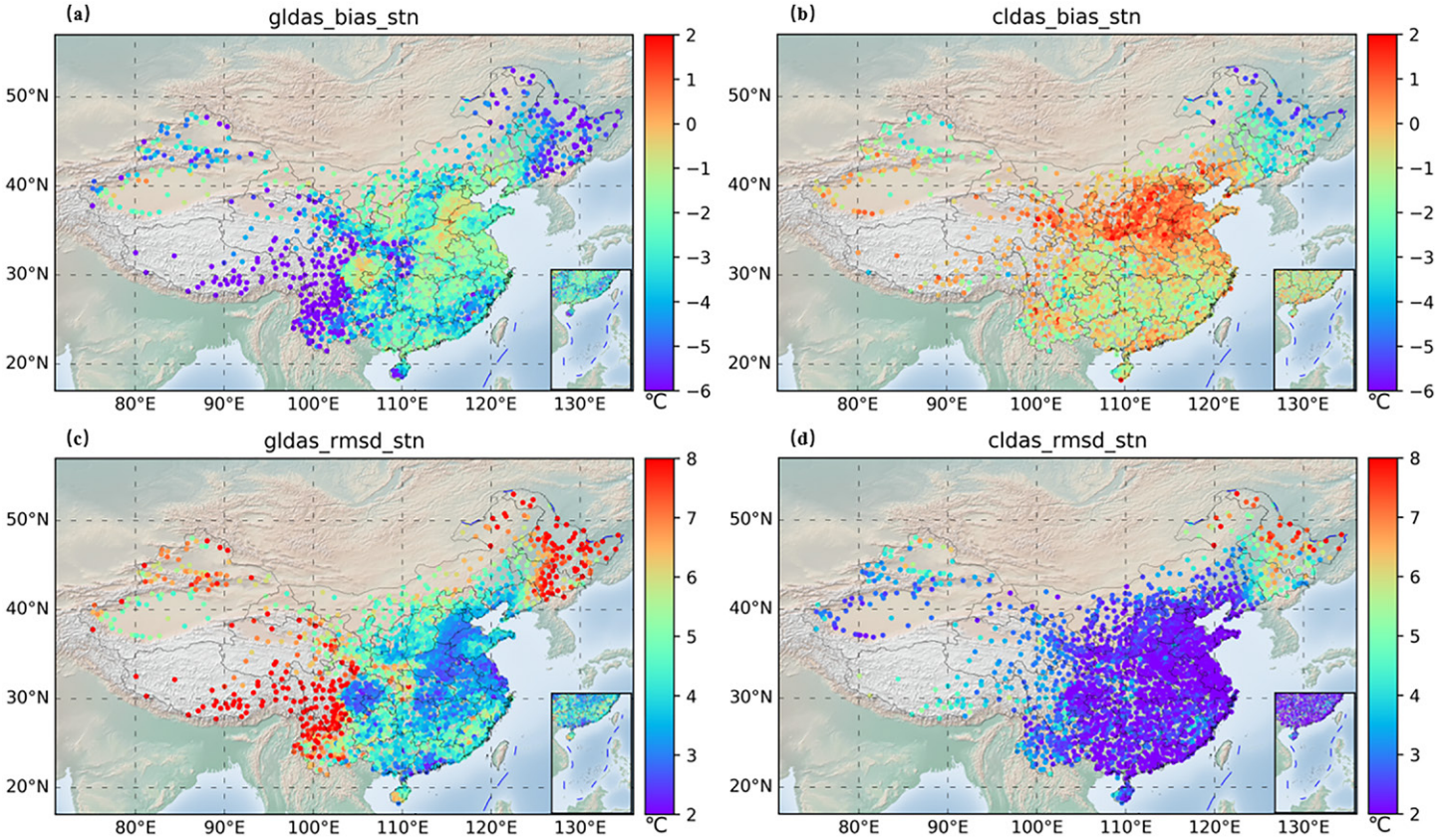

Fig. 8. The (a),(b) bias and (c),(d) root-mean-square deviation of the soil surface temperature in CLDAS and GLDAS. This figure was provided by Chunxiang Shi from the CMA.

simulate the TP land–air flux more reasonably, and the cold bias of the TP surface temperature has been reduced (Wu et al. 2021). In addition, the precipitation bias on the southern slope of the TP has been further reduced by approximately 30% (Bao and Li 2020; He et al. 2019a). The probability distribution characteristics of extreme hourly precipitation in slope areas and the diurnal cycles of precipitation in the Asian monsoon region are simulated better in FGOALS-f3-H than most CMIP6 models (S. He et al. 2019; Li et al. 2021b; Chen et al. 2022).

FGOALS-f3-L/H has participated in multiple inter-model comparison projects, including CMIP6's Diagnostic, Evaluation and Characterization of Klima (DECK) experiment, the Global Monsoons Model Intercomparison Project (GMMIP), and the High Resolution Model Intercomparison Project (HighResMIP) (He et al. 2020). These datasets are available through the ESG node (detailed in Table 4). Then, a subseasonal-to-seasonal (S2S) prediction system was established based on the updated model (Li et al. 2021a). The S2S prediction system releases forecast information on temperature, precipitation, and circulation anomalies over the TP in real time, and is now operational at the National Climate Center of the CMA and the Information Center of the Ministry of Water Resources in China.

Summary and perspectives

Since the launch of LASTPIC, many encouraging achievements have been made. For the first time, an integrated observation network has been established to reveal the land–atmosphere coupled processes in the near-surface layer, boundary layer, troposphere, and stratosphere over the TP. Based on the integrated network platform, a long-term hourly dataset of integrated land–atmosphere interaction observations on the TP (2005–16) has been collected and released. Furthermore, effective international cooperation has been carried out to provide new evidence that the TP acts as an important pathway for troposphere–stratosphere interaction. In addition, research has indicated that the TP's heating, rather than its role

Table 4. Download links of CMIP6 experiments derived from FGOALS-f3-L/H.

CMIP6 project	Experiment	Download link
DECK (FGOALS-f3-L)	piControl	http://doi.org/10.22033/ESGF/CMIP6.3447
	abrupt-4 × CO_2	http://doi.org/10.22033/ESGF/CMIP6.3176
	1pctCO_2	http://doi.org/10.22033/ESGF/CMIP6.3054
	amip	http://doi.org/10.22033/ESGF/CMIP6.3182
	historical	http://doi.org/10.22033/ESGF/CMIP6.3355
GMMIP (FGOALS-f3-L)	amip-hist	http://doi.org/10.22033/ESGF/CMIP6.3194
	amip-hld	http://doi.org/10.22033/ESGF/CMIP6.3197
	amip-TIP	http://doi.org/10.22033/ESGF/CMIP6.3186
	amip-TIP-nosh	http://doi.org/10.22033/ESGF/CMIP6.3189
HighResMIP (FGOALS-f3-H)	highresSST-present	http://doi.org/10.2022033/ESGF/CMIP6.203312
	highresSST-future	http://doi.org/10.2022033/ESGF/CMIP6.203308
HighResMIP (FGOALS-f3-L)	highresSST-present	http://doi.org/10.2022033/ESGF/CMIP6.2012009
	highresSST-future	http://doi.org/10.2022033/ESGF/CMIP6.2012007

as a thermal isolator separating tropical and extratropical air masses, is key for the formation of the ASM circulation, from the perspectives of energy, potential vorticity, and angular momentum conservation theories. Significant connections between the TP thermal forcing and SST anomalies in different oceans have been revealed, showing marked seasonality, while the TP can affect the generation of the remote AMOC according to findings in paleoclimatic studies. LASTPIC is also committed to observation assimilation and model development. In this respect, LASTPIC has contributed to the establishment of the CMA data assimilation system, CLDAS-V2.0, and a corresponding real-time product dataset. An updated version of a climate system model, i.e., FGOALS-f3-L/H, shows great improvements in the simulation of precipitation and temperature over the TP and its surrounding areas.

Although new features in surface physical processes and substance exchange between the troposphere and stratosphere in the UTLS layer have been revealed, how these processes occurring at the bottom and top of the troposphere are coupled is still unclear. Besides, how aerosols, cloud, and radiation over the TP interact and affect local and regional precipitation requires in-depth investigations. Furthermore, the connection in snow cover between Eurasian and the TP still needs to be explored. Therefore, a rational top-down design from the scientific committee, as well as comprehensive interdisciplinary efforts, efficient cooperation and integration among individual projects along with international cooperation are necessary for the efficient implementation of the LASTPIC program in the future.

Acknowledgments. This work was supported by the National Natural Science Foundation of China (Grants 91937302, 41730963, 92037000, 42030602, 41725018, and 42122035).

Data availability statement. No datasets were generated or analyzed during the current study.

References

Bao, Q., and J. Li, 2020: Progress in climate modeling of precipitation over the Tibetan Plateau. *Natl. Sci. Rev.*, **7**, 486–487, https://doi.org/10.1093/nsr/nwaa006.

Bian, J., D. Li, Z. Bai, Q. Li, D. Lyu, and X. Zhou, 2020: Transport of Asian surface pollutants to the global stratosphere from the Tibetan Plateau region during the Asian summer monsoon. *Natl. Sci. Rev.*, **7**, 516–533, https://doi.org/10.1093/nsr/nwaa005.

Bolin, B., 1950: On the influence of the Earth's orography on the general character of the westerlies. *Tellus*, **2**, 184–195, https://doi.org/10.3402/tellusa.v2i3.8547.

Boos, W. R., and Z. Kuang, 2010: Dominant control of the South Asian monsoon by orographic insulation versus plateau heating. *Nature*, **463**, 218–222, https://doi.org/10.1038/nature08707.

Chen, G., W.-C. Wang, Q. Bao, and J. Li, 2022: Evaluation of simulated cloud diurnal variation in CMIP6 climate models. *J. Geophys. Res. Atmos.*, **127**, e2021JD036422, https://doi.org/10.1029/2021JD036422.

Chen, L. X., 1999: China–Japan cooperative research on Asian monsoon mechanisms. Chinese Academy of Meteorological Sciences Annual Rep., 26–28.

Cheng, X., Y. Li, and L. Xu, 2016: An analysis of an extreme rainstorm caused by the interaction of the Tibetan Plateau vortex and the Southwest China vortex from an intensive observation. *Meteor. Atmos. Phys.*, **128**, 373–399, https://doi.org/10.1007/s00703-015-0420-2.

Cui, Y. F., A. Duan, Y. Liu, and G. Wu, 2015: Interannual variability of the spring atmospheric heat source over the Tibetan Plateau forced by the North Atlantic SSTA. *Climate Dyn.*, **45**, 1617–1634, https://doi.org/10.1007/s00382-014-2417-9.

Duan, A. M., and G. X. Wu, 2008: Weakening trend in the atmospheric heat source over the Tibetan Plateau during recent decades. Part I: Observations. *J. Climate*, **21**, 3149–3164, https://doi.org/10.1175/2007JCLI1912.1.

——, M. Wang, Y. Lei, and Y. Cui, 2013: Trends in summer rainfall over China associated with the Tibetan Plateau sensible heat source during 1980–2008. *J. Climate*, **26**, 261–275, https://doi.org/10.1175/JCLI-D-11-00669.1.

——, R. Sun, and J. He, 2017: Impact of surface sensible heating over the Tibetan Plateau on the western Pacific subtropical high: A land–air–sea interaction perspective. *Adv. Atmos. Sci.*, **34**, 157–168, https://doi.org/10.1007/s00376-016-6008-z.

Fallah, B., U. Cubasch, K. Prömmel, and S. Sodoudi, 2016: A numerical model study on the behaviour of Asian summer monsoon and AMOC due to orographic forcing of Tibetan Plateau. *Climate Dyn.*, **47**, 1485–1495, https://doi.org/10.1007/s00382-015-2914-5.

Fan, Q., J. C. Bian, and L. L. Pan, 2017: Stratospheric entry point for upper-tropospheric air within the Asian summer monsoon anticyclone. *Sci. China Earth Sci.*, **60**, 1685–1693, https://doi.org/10.1007/s11430-016-9073-5.

Fu, Y., and Coauthors, 2020: Land-surface processes and summer-cloud-precipitation characteristics in the Tibetan Plateau and their effects on downstream weather: A review and perspective. *Natl. Sci. Rev.*, **7**, 500–515, https://doi.org/10.1093/nsr/nwz226.

Gao, W., L. Liu, J. Li, and C. Lu, 2018: The microphysical properties of convective precipitation over the Tibetan Plateau by a subkilometer resolution cloud-resolving simulation. *J. Geophys. Res. Atmos.*, **123**, 3212–3227, https://doi.org/10.1002/2017JD027812.

Gu, Y., H. Liao, and J. Bian, 2016: Summertime nitrate aerosol in the upper troposphere and lower stratosphere over the Tibetan Plateau and the South Asian summer monsoon region. *Atmos. Chem. Phys.*, **16**, 6641–6663, https://doi.org/10.5194/acp-16-6641-2016.

Han, C., Y. Ma, X. Chen, and Z. Su, 2017: Trends of land surface heat fluxes on the Tibetan Plateau from 2001 to 2012. *Int. J. Climatol.*, **37**, 4757–4767, https://doi.org/10.1002/joc.5119.

Han, S., C. Shi, B. Xu, S. Sun, T. Zhang, L. Jiang, and X. Liang, 2019: Development and evaluation of hourly and kilometer resolution retrospective and real-time Surface Meteorological Blended Forcing Dataset (SMBFD) in China. *J. Meteor. Res.*, **33**, 1168–1181, https://doi.org/10.1007/s13351-019-9042-9.

He, B., G. Wu, Y. Liu, and Q. Bao, 2015: Astronomical and hydrological perspective of mountain impacts on the Asian summer monsoon. *Sci. Rep.*, **5**, 17586, https://doi.org/10.1038/srep17586.

——, and Coauthors, 2019a: CAS FGOALS-f3-L model datasets for CMIP6 historical Atmospheric Model Intercomparison Project simulation. *Adv. Atmos. Sci.*, **36**, 771–778, https://doi.org/10.1007/s00376-019-9027-8.

——, Y. Liu, G. Wu, Z. Wang, and Q. Bao, 2019b: The role of air–sea interactions in regulating the thermal effect of the Tibetan–Iranian Plateau on the Asian summer monsoon. *Climate Dyn.*, **52**, 4227–4245, https://doi.org/10.1007/s00382-018-4377-y.

——, and Coauthors, 2020: CAS FGOALS-f3-L model dataset descriptions for CMIP6 DECK experiments. *Atmos. Oceanic Sci. Lett.*, **13**, 582–588, https://doi.org/10.1080/16742834.2020.1778419.

——, C. Sheng, G. Wu, Y. Liu, and Y. Tang, 2022: Quantification of seasonal and interannual variations of the Tibetan Plateau surface thermodynamic forcing based on the potential vorticity. *Geophys. Res. Lett.*, **49**, e2021GL097222, https://doi.org/10.1029/2021GL097222.

He, S., J. Yang, Q. Bao, L. Wang, and B. Wang, 2019: Fidelity of the observational/reanalysis datasets and global climate models in representation of extreme precipitation in East China. *J. Climate*, **32**, 195–212, https://doi.org/10.1175/JCLI-D-18-0104.1.

Hsu, H. H., and X. Liu, 2003: Relationship between the Tibetan Plateau heating and East Asian summer monsoon rainfall. *Geophys. Res. Lett.*, **30**, 2066, https://doi.org/10.1029/2003GL017909.

Hu, J., and A. Duan, 2015: Relative contributions of the Tibetan Plateau thermal forcing and the Indian Ocean sea surface temperature basin mode to the interannual variability of the East Asian summer monsoon. *Climate Dyn.*, **45**, 2697–2711, https://doi.org/10.1007/s00382-015-2503-7.

Hu, L., D. Deng, S. Gao, and X. Xu, 2016: The seasonal variation of Tibetan convective systems: Satellite observation. *J. Geophys. Res. Atmos.*, **121**, 5512–5525, https://doi.org/10.1002/2015JD024390.

Lee, W.-L., K. N. Liou, and C. Wang, 2013: Impact of 3-D topography on surface radiation budget over the Tibetan Plateau. *Theor. Appl. Climatol.*, **113**, 95–103, https://doi.org/10.1007/s00704-012-0767-y.

Lelieveld, J., and Coauthors, 2018: The South Asian monsoon—Pollution pump and purifier. *Science*, **361**, 270–273, https://doi.org/10.1126/science.aar2501.

Li, D., and Coauthors, 2020: Dehydration and low ozone in the tropopause layer over the Asian monsoon caused by tropical cyclones: Lagrangian transport calculations using ERA-Interim and ERA5 reanalysis data. *Atmos. Chem. Phys.*, **20**, 4133–4152, https://doi.org/10.5194/acp-20-4133-2020.

Li, J., and Coauthors, 2021a: Dynamical seasonal prediction of tropical cyclone activity using the FGOALS-f2 ensemble prediction system. *Wea. Forecasting*, **36**, 1759–1778, https://doi.org/10.1175/WAF-D-20-0189.1.

——, Z. Sun, Y. Liu, Q. You, G. Chen, and Q. Bao, 2021b: Top-of-atmosphere radiation budget and cloud radiative effects over the Tibetan Plateau and adjacent monsoon regions from CMIP6 simulations. *J. Geophys. Res. Atmos.*, **126**, e2020JD034345, https://doi.org/10.1029/2020JD034345.

Li, X., and Coauthors, 2020: CASEarth poles big data for the three poles. *Bull. Amer. Meteor. Soc.*, **101**, E1475–E1491, https://doi.org/10.1175/BAMS-D-19-0280.1.

Liu, Y., Z. Wang, H. Zhuo, and G. Wu, 2017: Two types of summertime heating over Asian large-scale orography and excitation of potential-vorticity forcing II. Sensible heating over Tibetan-Iranian Plateau. *Sci. China Earth Sci.*, **60**, 733–744, https://doi.org/10.1007/s11430-016-9016-3.

——, M. Lu, H. Yang, A. Duan, B. He, S. Yang, and G. Wu, 2020: Land–atmosphere–ocean coupling associated with the Tibetan Plateau and its climate impacts. *Natl. Sci. Rev.*, **7**, 534–552, https://doi.org/10.1093/nsr/nwaa011.

Lu, M., S. Yang, Z. Li, B. He, S. He, and Z. Wang, 2018: Possible effect of the Tibetan Plateau on the "upstream" climate over west Asia, North Africa, south

Europe and the North Atlantic. *Climate Dyn.*, **51**, 1485–1498, https://doi.org/10.1007/s00382-017-3966-5.

——, B. Huang, Z. Li, S. Yang, and Z. Wang, 2019: Role of Atlantic air–sea interaction in modulating the effect of Tibetan Plateau heating on the upstream climate over Afro-Eurasia–Atlantic regions. *Climate Dyn.*, **53**, 509–519, https://doi.org/10.1007/s00382-018-4595-3.

Ma, J., and Coauthors, 2019: Modelling the aerosol chemical composition of the tropopause over the Tibetan Plateau during the Asian summer monsoon. *Atmos. Chem. Phys.*, **19**, 11 587–11 612, https://doi.org/10.5194/acp-19-11587-2019.

Ma, Y., H. Ishikawa, O. Tsukamoto, M. Menenti, Z. Su, T. Yao, T. Koike, and T. Yasunari, 2003: Regionalization of surface fluxes over heterogeneous landscape of the Tibetan Plateau by using satellite remote sensing data. *J. Meteor. Soc. Japan*, **81**, 277–293, https://doi.org/10.2151/jmsj.81.277.

——, and Coauthors, 2005: Diurnal and inter-monthly variation of land surface heat fluxes over the central Tibetan Plateau area. *Theor. Appl. Climatol.*, **80**, 259–273, https://doi.org/10.1007/s00704-004-0104-1.

——, and Coauthors, 2006: Experimental study of energy and water cycle in Tibetan Plateau-the progress introduction on the study of GAME/Tibet and CAMP/Tibet (in Chinese). *Plateau Meteor.*, **25**, 344–351.

——, S. Kang, L. Zhu, B. Xu, L. Tian, and T. Yao, 2008: Tibetan Observation and Research Platform: Atmosphere–land interaction over a heterogeneous landscape. *Bull. Amer. Meteor. Soc.*, **89**, 1487–1492, https://doi.org/10.1175/1520-0477-89.10.1469.

——, and Coauthors, 2011: Third Pole Environment (TPE) program: A new base for the study of atmosphere–land interaction over the heterogeneous landscape of the Tibetan Plateau and surrounding areas. *IAHS Publ.*, **343**, 110–117.

——, and Coauthors, 2017: Monitoring and modeling the Tibetan Plateau's climate system and its impact on East Asia. *Sci. Rep.*, **7**, 44574, https://doi.org/10.1038/srep44574.

Nan, S., P. Zhao, and J. Chen, 2019: Variability of summertime Tibetan tropospheric temperature and associated precipitation anomalies over the central-eastern Sahel. *Climate Dyn.*, **52**, 1819–1835, https://doi.org/10.1007/s00382-018-4246-8.

Park, M., W. J. Randel, L. K. Emmons, and N. J. Livesey, 2009: Transport pathways of carbon monoxide in the Asian summer monsoon diagnosed from Model of Ozone and Related Tracers (MOZART). *J. Geophys. Res.*, **114**, D08303, https://doi.org/10.1029/2008JD010621.

Qiu, J., 2013: Monsoon melee. *Science*, **340**, 1400–1401, https://doi.org/10.1126/science.340.6139.1400.

Schmitz, W. J., 1996: On the World Ocean circulation: Volume I—Some global features/North Atlantic circulation. Woods Hole Oceanographic Institution Tech. Rep. WHOI-96-03, 150 pp.

Sheng, C., B. He, G. X. Wu, Y. M. Liu, and S. Y. Zhang, 2022: Interannual influences of the surface potential vorticity forcing over the Tibetan Plateau on East Asian summer rainfall. *Adv. Atmos. Sci.*, **39**, 1050–1061, https://doi.org/10.1007/s00376-021-1218-4.

Sun, R., A. Duan, L. Chen, Y. Li, Z. Xie, and Y. Zhao, 2019: Interannual variability of the North Pacific mixed layer associated with the spring Tibetan Plateau thermal forcing. *J. Climate*, **32**, 3109–3130, https://doi.org/10.1175/JCLI-D-18-0577.1.

Sun, S., C. Shi, Y. Pan, L. Bai, B. Xu, T. Zhang, S. Han, and L. Jiang, 2020: Applicability assessment of the 1998–2018 CLDAS multi-source precipitation fusion dataset over China. *J. Meteor. Res.*, **34**, 879–892, https://doi.org/10.1007/s13351-020-9101-2.

Tao, S. Y., S. Luo, and H. Zhang, 1986: The Qinghai–Xizang Plateau Meteorological Experiment (QXPMEX) May–August 1979. *Proc. Int. Symp. on the Qinghai–Xizang Plateau and Mountain Meteorology*, Beijing, China, Amer. Meteor. Soc., 3–13.

Vernier, J. P., L. W. Thomason, and J. Kar, 2011: CALIPSO detection of an Asian tropopause aerosol layer. *Geophys. Res. Lett.*, **38**, L07804, https://doi.org/10.1029/2010GL046614.

Wang, Z., A. Duan, and S. Yang, 2018: Potential regulation on the climatic effect of Tibetan Plateau heating by tropical air–sea coupling in regional models. *Climate Dyn.*, **52**, 1685–1694, https://doi.org/10.1007/s00382-018-4218-z.

Wu, G. X., and Y. S. Zhang, 1998: Tibetan Plateau forcing and the timing of the monsoon onset over South Asian and the South China Sea. *Mon. Wea. Rev.*, **126**, 913–927, https://doi.org/10.1175/1520-0493(1998)126<0913:TPFATT>2.0.CO;2.

——, W. P. Li, H. Guo, H. Liu, J. S. Xue, and Z. Z. Wang, 1997: Sensible heat driven air–pump over the Tibetan Plateau and its impacts on the Asian summer monsoon. *Collections on the Memory of Dr. Zhao Jiuzhang*, D. Ye, Ed., Chinese Science Press, 116–126.

——, and Coauthors, 2007: The influence of the mechanical and thermal forcing of the Tibetan Plateau on the Asian climate. *J. Hydrometeor.*, **8**, 770–789, https://doi.org/10.1175/JHM609.1.

——, Y. Liu, B. He, Q. Bao, A. M. Duan, and F. F. Jin, 2012a: Thermal controls on the Asian summer monsoon. *Sci. Rep.*, **2**, 404, https://doi.org/10.1038/srep00404.

——, ——, B. W. Dong, X. Liang, A. Duan, Q. Bao, and J. Yu, 2012b: Revisiting Asian monsoon formation and change associated with Tibetan Plateau forcing: I. Formation. *Climate Dyn.*, **39**, 1169–1181, https://doi.org/10.1007/s00382-012-1334-z.

——, and Coauthors, 2015: Tibetan Plateau climate dynamics: Recent research progress and outlook. *Natl. Sci. Rev.*, **2**, 100–116, https://doi.org/10.1093/nsr/nwu045.

——, B. He, A. Duan, Y. Liu, and W. Yu, 2017: Formation and variation of the atmospheric heat source over the Tibetan Plateau and its climate effects. *Adv. Atmos. Sci.*, **34**, 1169–1184, https://doi.org/10.1007/s00376-017-7014-5.

Wu, Y., Y. Liu, J. Li, Q. Bao, B. He, L. Wang, X. Wang, and J. Li, 2021: Analysis of surface temperature bias over the Tibetan Plateau in the CAS FGOALS-f3-L model. *Atmos. Ocean. Sci. Lett.*, **14**, 100012, https://doi.org/10.1016/j.aosl.2020.100012.

Xu, X., and Coauthors, 2008: A new integrated observational system over the Tibetan Plateau. *Bull. Amer. Meteor. Soc.*, **89**, 1492–1496, https://doi.org/10.1175/1520-0477-89.10.1469.

Yan, Y., and Y. Liu, 2019: Vertical structures of convective and stratiform clouds in boreal summer over the Tibetan Plateau and its neighboring regions. *Adv. Atmos. Sci.*, **36**, 1089–1102, https://doi.org/10.1007/s00376-019-8229-4.

Yanai, M., and G.-X. Wu, 2006: Effects of the Tibetan Plateau. *The Asian Monsoon*, B. Wang, Ed., Springer, 513–549.

Yang, H., and Q. Wen, 2020: Investigating the role of the Tibetan Plateau in the formation of Atlantic meridional overturning circulation. *J. Climate*, **33**, 3585–3601, https://doi.org/10.1175/JCLI-D-19-0205.1.

Yang, K., and C. Wang, 2019a: Seasonal persistence of soil moisture anomalies related to freeze–thaw over the Tibetan Plateau and prediction signal of summer precipitation in eastern China. *Climate Dyn.*, **53**, 2411–2424, https://doi.org/10.1007/s00382-019-04867-1.

——, and ——, 2019b: Water storage effect of soil freeze-thaw process and its impacts on soil hydro-thermal regime variations. *Agric. For. Meteor.*, **265**, 280–294, https://doi.org/10.1016/j.agrformet.2018.11.011.

——, X. Guo, and B. Wu, 2011: Recent trends in surface sensible heat flux on the Tibetan Plateau. *Sci. China Earth Sci.*, **54**, 19–28, https://doi.org/10.1007/s11430-010-4036-6.

Yao, T., and Coauthors, 2012: Third Pole Environment (TPE). *Environ. Dev.*, **3**, 52–64, https://doi.org/10.1016/j.envdev.2012.04.002.

Yeh, T. C., 1950: The circulation of the high troposphere over China in the winter of 1945–1946. *Tellus*, **2**, 173–183, https://doi.org/10.3402/tellusa.v2i3.8548.

Yu, P., and Coauthors, 2017: Efficient transport of tropospheric aerosol into the stratosphere via the Asian summer monsoon anticyclone. *Proc. Natl. Acad. Sci. USA*, **114**, 6972–6977, https://doi.org/10.1073/pnas.1701170114.

Yu, W., Y. Liu, X. Yang, and G. Wu, 2018: The interannual and decadal variation characteristics of the surface sensible heating at different elevations over the Qinghai-Tibetan Plateau and attribution analysis. *Plateau Meteor.*, **37**, 1161–1176.

——, ——, ——, ——, B. He, J. Li, and Q. Bao, 2021: Impact of North Atlantic SST and Tibetan Plateau forcing on seasonal transition of springtime South Asian monsoon circulation. *Climate Dyn.*, **56**, 559–579, https://doi.org/10.1007/s00382-020-05491-0.

——, and Coauthors, 2022: Potential impact of spring thermal forcing over the Tibetan Plateau on the following winter El Niño–Southern Oscillation. *Geophys. Res. Lett.*, **49**, e2021GL097234, https://doi.org/10.1029/2021GL097234.

Zhang, Q., J. Jin, X. Wang, P. Budy, N. Barrett, and S. E. Null, 2019: Improving lake mixing process simulations in the Community Land Model by using K profile parameterization. *Hydrol. Earth Syst. Sci.*, **23**, 4969–4982, https://doi.org/10.5194/hess-23-4969-2019.

Zhao, C., L. Liu, Q. Wang, Y. Qiu, Y. Wang, and X. Wu, 2017: MMCR-based characteristic properties of non-precipitating cloud liquid droplets at Naqu site over Tibetan Plateau in July 2014. *Atmos. Res.*, **190**, 68–76, https://doi.org/10.1016/j.atmosres.2017.02.002.

Zhao, P., and Coauthors, 2018: The third atmospheric scientific experiment for understanding the Earth–atmosphere coupled system over the Tibetan Plateau and its effects. *Bull. Amer. Meteor. Soc.*, **99**, 757–776, https://doi.org/10.1175/BAMS-D-16-0050.1.

Zhao, Y., A. Duan, and G. Wu, 2018: Interannual variability of late-spring circulation and diabatic heating over the Tibetan Plateau associated with Indian Ocean forcing. *Adv. Atmos. Sci.*, **35**, 927–941, https://doi.org/10.1007/s00376-018-7217-4.

——, X. Xu, L. Liu, R. Zhang, H. Xu, Y. Wang, and J. Li, 2019a: Effects of convection over the Tibetan Plateau on rainstorms downstream of the Yangtze River basin. *Atmos. Res.*, **219**, 24–35, https://doi.org/10.1016/j.atmosres.2018.12.019.

——, ——, Z. Ruan, B. Chen, and F. Wang, 2019b: Precursory strong-signal characteristics of the convective clouds of the central Tibetan Plateau detected by radar echoes with respect to the evolutionary processes of an eastward-moving heavy rainstorm belt in the Yangtze River basin. *Meteor. Atmos. Phys.*, **131**, 697–712, https://doi.org/10.1007/s00703-018-0597-2.

Zhong, L., Y. Ma, Y. Xue, and S. Piao, 2019a: Climate change trends and impacts on vegetation greening over the Tibetan Plateau. *J. Geophys. Res. Atmos.*, **124**, 7540–7552, https://doi.org/10.1029/2019JD030481.

——, ——, Z. Hu, Y. Fu, Y. Hu, X. Wang, M. Cheng, and N. Ge, 2019b: Estimation of hourly land surface heat fluxes over the Tibetan Plateau by the combined use of geostationary and polar-orbiting satellites. *Atmos. Chem. Phys.*, **19**, 5529–5541, https://doi.org/10.5194/acp-19-5529-2019.

Zhu, L., J. Jin, and Y. Liu, 2020: Modeling the effects of lakes in the Tibetan Plateau on diurnal variations of regional climate and their seasonality. *J. Hydrometeor.*, **21**, 2523–2536, https://doi.org/10.1175/JHM-D-20-0091.1.